Global Biogeochemical Cycles

RESEARCH ARTICLE
10.1029/2020GB006677

Special Section:
Fire in the Earth System

Interaction of Fire, Vegetation, and Climate in Tropical Ecosystems: A Multiproxy Study Over the Past 22,000 Years

Y. Ruan[1], M. Mohtadi[1], L. M. Dupont[1], D. Hebbeln[1], S. van der Kaars[2,3,4], E. C. Hopmans[5], S. Schouten[5,6], E. J. Hyer[7], and E. Schefuß[1]

[1]MARUM—Center for Marine Environmental Sciences, University of Bremen, Bremen, Germany, [2]School of Earth, Atmosphere, and Environment, Monash University, Clayton, Victoria, Australia, [3]Cluster Earth and Climate, Department of Earth Sciences, Faculty of Sciences, Vrije Universiteit, Amsterdam, The Netherlands, [4]Department of Palynology and Climate Dynamics, Albrecht-von-Haller Institute for Plant Sciences, University of Göttingen, Göttingen, Germany, [5]Department of Microbiology and Biogeochemistry, NIOZ Royal Netherlands Institute for Sea Research, Utrecht University, Texel, The Netherlands, [6]Department of Earth Sciences, Utrecht University, Utrecht, The Netherlands, [7]Naval Research Laboratory, Marine Meteorology Division, Monterey, CA, USA

Key Points:
- Microcharcoal reflects regional fire occurrence, while the ratio between two novel molecular markers reflects past fire intensity
- Rainfall seasonality controlled both fire regime and vegetation
- Fires of different frequencies and intensities were capable of either stabilizing or destabilizing savannah/rainforest vegetation

Supporting Information:
- Supporting Information S1

Correspondence to:
Y. Ruan,
yruan@marum.de

Citation:
Ruan, Y., Mohtadi, M., Dupont, L. M., Hebbeln, D., van der Kaars, S., Hopmans, E. C., et al. (2020). Interaction of fire, vegetation, and climate in tropical ecosystems: A multiproxy study over the past 22,000 years. *Global Biogeochemical Cycles*, *34*, e2020GB006677. https://doi.org/10.1029/2020GB006677

Received 22 MAY 2020
Accepted 16 OCT 2020
Accepted article online 21 OCT 2020

Abstract Fire causes dramatic energy and matter exchanges between biosphere and atmosphere on a regional to global scale. Predicting fires, however, is hindered by the complex interplay of fire, climate, and vegetation. Paleo-fire records provide critical information beyond instrumental records that cover only the past few decades and may be used to assess the role of fire in large-scale and long-term environmental changes. Here we present a 22,000-year multiproxy record of fire regime from a sediment core retrieved offshore South Java, Indonesia. We use microcharcoal in combination with two molecular markers of burning, levoglucosan and polycyclic aromatic hydrocarbons, to reconstruct fire occurrence as well as fire intensity in the past. We show that fire occurrence and intensity were high during the Last Glacial Maximum (LGM; around 21,000 years ago) and low during the Heinrich Stadial 1 and the early Holocene. Both fire regime and vegetation in tropical regions with high annual rainfall were primarily controlled by rainfall seasonality. However, fire additionally stabilized the savannah (rainforest)-dominated ecosystem during the LGM (early Holocene) but caused transitions between the two vegetation types during the deglaciation and the late Holocene.

1. Introduction

Fire is a ubiquitous component of almost every terrestrial ecosystem on Earth (Bowman et al., 2009). Emissions from biomass burning such as aerosols, greenhouse gases, and chemically active gases change the chemical composition of the atmosphere and play a significant role in regional and global biogeochemical cycles (Ramanathan et al., 2001; Santín et al., 2016). Fire frequency and fire intensity are two important fire regime characteristics in describing fire patterns (Bond & Keeley, 2005; Gill, 1975). They are related to both vegetation type and hydroclimate (Archibald et al., 2013; Murphy & Bowman, 2012). While fires in tropical moist broadleaf forests are predominantly of low intensity (burning temperature) and low to intermediate frequency, tropical grassland fires are more frequent and tend to reach higher intensity (burning temperature) (Archibald et al., 2013). Modern observations in the tropics reveal more frequent fires in years with extended dry seasons (Van der Werf et al., 2008). Fire experiments in savannah ecosystems show high intensity fires when the moisture content of fuel is low (Govender et al., 2006). Therefore, climate and vegetation are two important factors in understanding how fire interacts with environmental changes, although only about half of the existing studies about fire feedbacks tackle both factors (Archibald et al., 2018). Paleo-fire records are essential in providing data beyond the timeframe of modern observations and to assess the role of fire in large-scale and long-term ecological changes. However, multiproxy paleo-records integrating fire, climate, and vegetation are sparse (Dupont & Schefuß, 2018; Shanahan et al., 2016).

Changes in fire regime are often not resolved in paleo-records (Archibald et al., 2018; Han et al., 2016). Charcoal, commonly used as a proxy to indicate past fire activity, is a carbonaceous material produced by incomplete combustion of biomass with temperatures between 280°C and 500°C (Whitlock & Larsen, 2002). Microcharcoal abundance in marine sediments reflects general fire occurrence on a

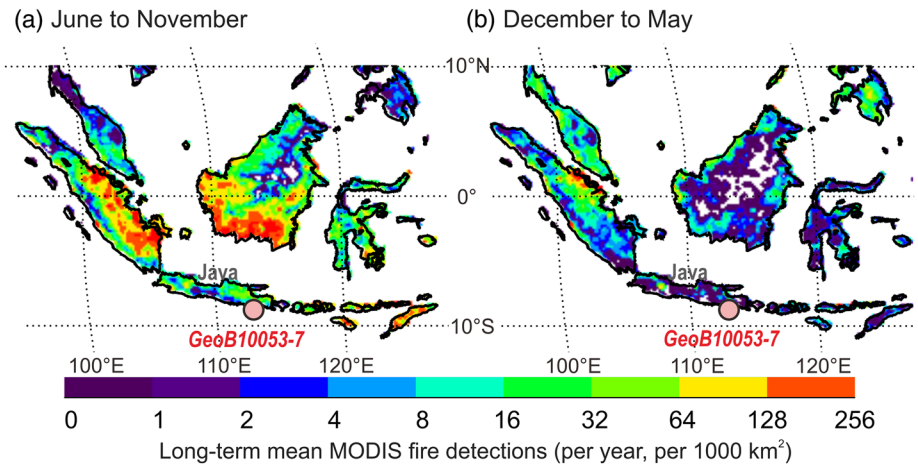

Figure 1. Seasonal distribution of MODIS active fire hot spot: (a) for June to November (dry season), (b) for December to May (wet season). Long-term mean results from 2003 to 2018 are based on the fire products of Aqua MODIS Collection 6 (Giglio et al., 2016). Location of the sediment core GeoB10053-7 (pink dot) is shown.

regional scale, representing fire frequency, intensity, and extent (Beaufort et al., 2003; Daniau et al., 2010, 2019). Combining sedimentary charcoal record with combustion-derived molecular markers, such as levoglucosan (a monosaccharide anhydrate compound) and/or polycyclic aromatic hydrocarbons (PAHs), is a promising new way of reconstructing fire intensity (Argiriadis et al., 2018; Battistel et al., 2017; Dietze et al., 2019; Miller et al., 2017; Schreuder et al., 2019; Schüpbach et al., 2015; Shanahan et al., 2016; Sikes et al., 2013). Levoglucosan (1,6-anhydro-β-D-glucopyranose), a product of cellulose combustion, is a tracer for biomass burning due to its high emission factor and specific pyrogenic sources (Bhattarai et al., 2019; Schkolnik & Rudich, 2006; Simoneit et al., 1999; Suciu et al., 2019). It is only formed at low burning temperatures (150–350°C) and, thus, reflects low intensity fires (Kuo et al., 2008). Pyrogenic PAHs are formed at a wider range of higher burning temperatures (200–700°C) (Keiluweit et al., 2012; Lu et al., 2009). According to an *in situ* forest fire emission study, more particle-associated PAHs are produced during the flaming phase of combustion (with higher burning intensity) than during the smoldering phase of combustion (with lower burning intenstiy), while higher emission of levoglucosan occurs during the smoldering phase than during the flaming phase (Wang et al., 2017).

Modern ecological studies show that tropical forest and savannah are two alternative stable states which can coexist under similar environmental conditions, despite distinct ecological structures, biodiversity, and carbon storage (Hirota et al., 2011; Staver et al., 2011). According to the alternative stable state theory, stabilizing feedbacks maintain these two ecosystems: High tree cover and rare fires are typical for tropical forest, while open canopy with grassy ground layer and frequent fires characterize the savannah (Murphy & Bowman, 2012; Ondei et al., 2017). Shifts between these two ecosystems occur if the feedback processes are disturbed (Murphy & Bowman, 2012). Several multidecadal fire-exclusion experiments show the tendency for forest species to invade and replace savannahs when fires are absent or of low frequency and/or intensity (Veenendaal et al., 2018, and references therein). In this study, we reconstruct 22,000 years of fire regime changes by analyzing microcharcoal, levoglucosan and PAHs from a sediment core. The accumulation rate of microcharcoal reflects general fire occurrence, while the two novel molecular markers of burning shed light on changes in fire intensity. The study area experienced shifts in rainfall seasonality and vegetation (savannah-rainforest transition) through the past 22,000 years (Ruan et al., 2019). This multiproxy study aims to evaluate the role of fire in the ecotone from savannah- to rainforest-dominated ecosystems in tropical regions on the time scale from the Last Glacial to the present.

2. Materials and Methods

2.1. Modern Fire Distribution in the Study Area

Modern fires in Java, Indonesia, display a distinct seasonal pattern as detected by satellite observations (Figure 1), with high fire occurrence during the dry season and low fire occurrence during the wet season,

since a sufficient amount of dry fuel for ignition is the prerequisite for fires (Reid et al., 2012). Thus, we assume a dry season biased production of microcharcoal particles and fire-induced molecular markers. Riverine discharge, the major transport process in wet areas, is postulated to bring microcharcoal and molecular markers deposited in soils or rivers of East Java into the marine environment year-round with peaks during the wet season. During the dry season transport by aerosols may play a role. The prevailing wind direction during the dry (fire) season (Figure 1a) is southeast (Kalnay et al., 1996); therefore, the inclusion of material from Australia cannot be ruled out but is expected to be minor due to the transport distance of over 1,500 km today and over 900 km during the Last Glacial Maximum (LGM) when lower sea level exposed the Sahul Shelf. The ~3,000 km long and up to 3,800 m high volcanic arc mountain ranges from Sumatra to Java serves as a barrier preventing the burning emissions of the exposed Sunda Shelf during the LGM from reaching our core location.

2.2. Site Description

Sediment core GeoB 10053-7 (8°40.59′S; 112°52.35′E, 1,375 m water depth; 750 cm core length; Figure 1) was retrieved off south Java, Indonesia, during the SO-184 "PABESIA" expedition in 2005 (Hebbeln & cruise participants, 2006). According to the previously published age model based on 19 accelerator mass spectrometry (AMS) ^{14}C dates (Mohtadi et al., 2011), the sediment core covers the past 22,000 years. The stable hydrogen and carbon isotope composition of long chain *n*-alkanes together with pollen data from this sediment core were reported by Ruan et al. (2019). Analyses of microcharcoal and fire-induced molecular markers (levoglucosan and PAHs) will be described here. For charcoal analysis, 34 sediment samples were collected at depth intervals of 3 to 40 cm. For molecular marker analysis, 74 samples were collected at depth intervals of 2 to 20 cm.

2.3. Microcharcoal Analysis

For each sample an amount between 4.8 and 6.0 ml of sediment was suspended in approximately 40 ml of tetra-sodium-pyrophosphate (±10%) then sieved over 200 and 7 μm screens, followed by hydrochloric acid (10%) treatment, heavy liquid separation (sodium-polytungstate, SG 2.0, 20 min at 2,000 rpm, twice), acetolysis, and sodium carbonate (20%) treatment. The resulting organic residues were mounted in glycerol on microscope slides sealed with paraffin wax. Charcoal particles >10 μm were counted along three evenly spaced transects in every slide, following a standard proccudure (e.g., Van der Kaars et al., 2000, 2017). To account for biases due to sediment rates, the accumulation rate of charcoal particles was calculated by multiplying the charcoal count (particles cm^{-3}) with the sedimentation rate (cm kyr^{-1}) based on the age model.

2.4. Analysis of PAHs

A DIONEX Accelerated Solvent Extractor (ASE 200) was used for lipid extractions with a mixture of dichloromethane:methanol (DCM:MeOH 9:1, v:v) at 1000 psi and 100°C (three cycles, 5 min each). An internal standard (2-Nonadecanone) was added to each sample prior to extraction. Saponification was carried out with 0.1 M KOH-solution. Neutral fractions were recovered by *n*-hexane. Further separation of the neutral fractions was achieved by a 5 cm silica gel column: subsequent elution with *n*-hexane, DCM, and DCM to MeOH (1:1, v:v) yielded the apolar, ketone and polar fractions, respectively. The ketone fractions, containing the PAHs, were dissolved in 50 μl dilute internal standard solution, that is, 1 ng/μl 2-Fluorofluorene (Sigma-Aldrich Co.) in toluene, before PAH analysis. We used an Agilent 7820A Gas Chromatograph (GC) equipped with an Rxi-PAH capillary column (40 m, 0.18 mm i.d., 0.07 μm) coupled to a 5977E Mass Selective Detector (MSD) quadrupole mass spectrometer to determine the concentrations of PAHs. Injection volume was 1 μl (splitless mode; 275°C); helium was used as carrier gas with a flow rate of 1.4 ml min^{-1}. GC oven temperature was programmed to 110°C for 1 min, then ramped to 210°C at 37°C per min, to 260°C at 3°C per min, to 350°C at 11°C per min and held for 8 min. The MSD transfer line was held at 280°C, and the ion source temperature was 230°C. Electron ionization was accomplished with an electron energy of 70 eV in single ion monitoring (SIM) mode (masses shown in Table 1).

Linearity of mass spectrometer performance was evaluated using standard solutions (a mixture of nine PAHs) (PAH Kit 610-N, SUPELCO) with seven concentration levels. Injections of PAHs of 0.05, 0.1, 0.5, 1, 2, 4, and 5 ng on column resulted in a linear response with $R^2 > 0.99$ for all individual PAHs (Table 1). Instrument performance and relative response factors (RRFs) for PAHs compared to 2-Fluorofluorene were

Table 1
PAH Name Abbreviations, Range and Linear Regression of Calibration Curves, Precision and Accuracy of Standards, and Reproducibility of Duplicates

PAH name and abbreviation	Qualitative ion (*m/z*)	Linear range (ng/μl)	Linear coefficient (%) ($n = 21$)	Precision of standard % ($n = 15$)	Accuracy of standard % ($n = 15$)	Relative difference of duplicate%
Benzo(*a*)anthracene (BaA)	228	0.05 – 5	99.5	1.9	1.2	4
Chrysene (Chry)	228	0.05 – 5	99.6	1.8	0.7	4
Benzo(*b/j/k*)fluoran-thene (BF)	252	0.05 – 5	99.2	2.7	1.1	4
Benzo(*a*)pyrene (BaP)	252	0.05 – 5	99.5	2.1	0.9	10
Indeno(1,2,3-*cd*)pyrene (IP)	276	0.05 – 5	99.1	1.8	0.5	8
Dibenzo(*a,h*)anth-racene (DBA)	278	0.05 – 5	99.5	2.6	1	6
Benzo(*g,h,i*)pery-lene (BghiP)	276	0.05 – 5	99.5	2.3	0.5	6

monitored by repetitive measurements of one standard mixture solution before, between and after samples. The precision and accuracy for each analyzed PAH are shown in Table 1.

$$Precision = \frac{SD_{measured\ conc}}{\overline{Conc}} \times 100\%$$

where $SD_{measured\ conc}$ is the standard deviation of measured concentrations of the standard; $\overline{Conc}$ is the average measured concentration of the standard.

$$Accuracy = \frac{\overline{Conc} - Conc}{Conc} \times 100\%$$

where *Conc* is the actual concentration of the standard.

We identified each peak according to the SIM mass (*m/z* shown in Table 1) and retention time of the standard mixture. Quantification was determined by comparing the peak area of the target compound to that of the internal standard (2-Fluorofluorene) and applying the RRFs. Duplicate measurements on five samples revealed an average relative difference between 4% for BaA/Chry/BF (name abbreviations shown in Table 1) and 10% for BaP (Table 1).

$$Relative\ difference = \frac{Conc_1 - Conc_2}{\overline{Conc}_{1,2}} \times 100\%$$

Relative difference was calculated as the difference of two measured concentrations ($Conc_1$ and $Conc_2$) divided by the average of the two ($\overline{Conc}_{1,2}$). To account for biases due to sediment properties and sediment rates, the accumulation rate of PAHs (ng cm^{-2} kyr^{-1}) was calculated by multiplying the concentration (ng g^{-1}) with the dry bulk density of the sediment (g cm^{-3}) and the sedimentation rate (cm kyr^{-1}) based on the age model.

2.5. Source of PAHs

PAHs are ubiquitous in the environment. Apart from incomplete combustion (pyrogenic PAHs), other origins include petroleum (petrogenic PAHs) and diagenesis of biogenic precursors (Lima et al., 2005, and references therein). Petrogenic PAHs enter the environment directly through either human-induced oil spill or natural oil seepage (Lima et al., 2005, and references therein). Biogenic PAHs occur as a localized source, and only types of PAHs not analyzed in this study are generated (perylene, phenanthrene homologs etc.) (Wakeham et al., 1980).

The suite of PAHs is always emitted as a mixture. Therefore, diagnostic ratios are commonly used to distinguish petrogenic and pyrogenic sources and to further identify emission sources of combustion (biomass or fossil fuels) (Tobiszewski & Namieśnik, 2012). Diagnostic ratios mostly involve pairs of PAHs which have the same molecular weight, similar physical and chemical properties, and undergo comparable environmental fates (Tobiszewski & Namieśnik, 2012). Pyrogenic input is inferred from an increase in the proportion of the less stable isomer relative to the more stable isomer compared to petrogenic input (Yunker et al., 2002). With the same molecular weight, Indeno(1,2,3-*cd*)pyrene (IP) is less stable than Benzo(*g,h,i*)perylene (BghiP);

thus, an increase in the IP/(IP + BghiP) ratio indicates more contribution from combustion than petroleum. Petrogenic input is generally featured by IP/(IP + BghiP) ratios <0.2 (Yunker et al., 2002).

2.6. Analysis of Levoglucosan

After the ASE extraction with a mixture of DCM:MeOH (9:1, v:v), the residual sediments were further extracted using a DIONEX Accelerated Solvent Extractor (ASE 200) with MeOH at 1,000 psi and 100°C (three cycles, 5 min each). The methanol extracts were passed over cotton wool to eliminate large salt particles. A known amount of deuterated (D7) levoglucosan (dLVG, Cambrige Isotope Laboratories, Inc.) (usually 0.25 ng) was added as an internal standard to 1/10 aliquot of each extract. The extracts were eluted over a small Na_2SO_4 Pasteur pipette column with dichloromethane to methanol (9:1, v:v) to further remove salt. After being dried under N_2, each extract was dissolved in acetonitrile: H_2O (95:5, v:v) and filtered through a polytetrafluoroethylene (PTFE) filter (0.45 μm; 13 mm diameter) before analysis.

Levoglucosan analysis was performed as described in detail by Schreuder et al. (2018). The extracts were analyzed using an Agilent 1290 Infinity Ultra-High Performance Liquid Chromatography (UHPLC) coupled to an Agilent 6230 Time-Of-Flight (TOF) mass spectrometer. Separation was achieved with two Aquity BEH amide columns (150 mm, 2.1 mm i.d., 1.7 μm, Waters Chromatography) in series with a 50 mm guard column. Linearity of mass spectrometer performance was evaluated using nine point standard curve; injections of levoglucosan (Sigma-Aldrich Co.) or dLVG of 12.5 pg, 25 pg, 50 pg, 125 pg, 250 pg, 0.5 ng, 1.25 ng, 2.5 ng, and 5 ng on column resulted in a linear response with $R^2 > 0.99$. Instrument performance and RRFs for levoglucosan compared to dLVG were monitored by repetitive measurements of one standard solution before, after and between samples. Quantification was based on peak integrations of mass chromatograms within 10 ppm mass accuracy using an exact mass of 161.0445 *m/z* for levoglucosan and 168.0884 *m/z* for dLVG. Duplicate measurements on 10% of all samples revealed an average relative difference of 2.5% for levoglucosan. To account for biases due to sediment properties and sediment rates, the accumulation rate of levoglucosan (ng cm^{-2} kyr^{-1}) was calculated by multiplying the concentration (ng g^{-1}) with the dry bulk density of the sediment (g cm^{-3}) and the sedimentation rate (cm kyr^{-1}) based on the age model.

To estimate the extraction loss of levoglucosan due to prior extraction using DCM:MeOH (9:1, v:v), we measured the levoglucosan amounts in the DCM:MeOH (9:1, v:v) extracts of 13 samples from the sediment core and compared each amount with that of the MeOH extract from the same sample. The extracts of DCM:MeOH (9:1, v:v) contain on average 17 ± 8% (average ± standard deviation, $n = 13$) of the levoglucosan amount in the MeOH extracts. This indicates that the MeOH extracts contain a major portion of the total levoglucosan concentrations in the samples. In order to correct for this loss due to prior DCM:MeOH (9:1, v:v) extractions, we calculated the total concentrations (Figure S1d in the supporting information) and accumulation rates (Figure 2d) of levoglucosan in the samples using the average and standard deviation above. We note the considerable variation in the levogucosan percentages in the DCM fraction, with a standard deviation of 8%. However, the DCM fraction is minor compared to the MeOH fraction: Lower amounts of levoglucosan are measured in the DCM fraction, are closer to the detection limit, and therefore expected to carry higher analytical errors than the MeOH fraction, which is a common analytical phenomenon.

2.7. Fire Regime Reconstruction and Comparison With Vegetation and Hydroclimatic Proxies

The ratio between levoglucosan and the pyrogenic PAHs (abbreviated as LVG/(LVG + PAHs) ratio) from marine sediments has the potential to reflect the intensity of source fires, because these two molecular markers share similar environmental fates before being deposited in marine sediments. The two types of compounds are emitted into the atmosphere mainly attached to particles from fires (Wang et al., 2017). Both undergo photochemical alterations in the atmosphere (Bhattarai et al., 2019; Lima et al., 2005) before dry deposition in the marine environment. An alternative transport route is via aerosol deposition in soils and subsequent river transport into the marine environment. In this regard, both types of compounds are transported similarly by river systems (Myers-Pigg et al., 2017). Particularly, the steep topography from the volcanic arc to the core site in East Java without a delta system favors relatively fast transport and sedimentary deposition of fire-induced molecular markers (Hunsinger et al., 2008). It is noteworthy that levoglucosan in marine sediments is prone to degradation at the seawater-sediment interface (Schreuder et al., 2018), which is substantially less for PAHs due to their more stable chemical structures. Such a degradation could bias the concentration of levoglucosan and its ratio to PAHs, if preservational conditions (e.g., oxygen

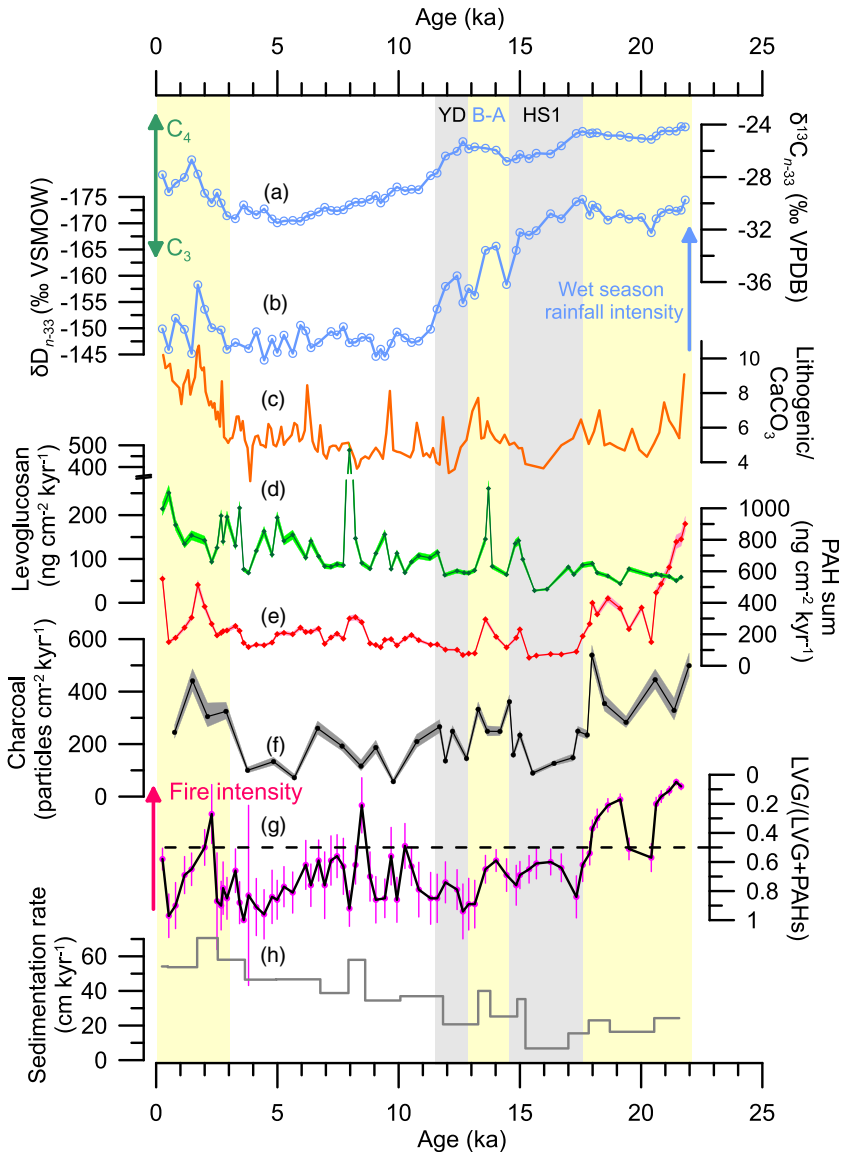

Figure 2. Comparison of various proxy records from sediment core GeoB10053-7. (a) The $\delta^{13}C$ values of the n-C_{33} alkane as proxy for lowland vegetation in East Java; C_4 grass expansion during LGM is shown (Ruan et al., 2019). (b) The ice volume adjusted δD values of the n-C_{33} alkane as proxy for wet season rainfall intensity in East Java lowlands (Ruan et al., 2019). (c) The ratio of lithogenic particles to calcium carbonate as a proxy for river runoff (Mohtadi et al., 2011). According to (b) and (c), rainfall seasonality in East Java lowlands was enhanced during the LGM, with a shorter but wetter rainy season. (d) Accumulation rates of levoglucosan with error ranges based on the determined extraction efficiency. The dark green dots show the levoglucosan accumulation rates of each methanol extract multiplied by 1.17. The error envelope represents the lower and upper limit of total levoglucosan accumulation rates, that is, accumulation rates of each methanol extract multiplied by 1.09 and 1.25, respectively. Note the break in the *Y* axis. (e) Accumulation rates of total PAHs with error ranges based on the relative difference of duplicate (Table 1). (f) Accumulation rates of microcharcoal particles with 95% confidence limits. The ratio of LVG/(LVG + PAHs) (g) reflects fire intensity. Vertical error bars are shown. (h) Sedimentation rate based on the age model (Mohtadi et al., 2011). Three vertical yellow bars show periods of peaks in microcharcoal accumulation rates, which correspond to the LGM, the Bølling-Allerød (B-A), and the late Holocene. Two vertical gray bars correspond to the Heinrich Stadial 1 (HS1) and the Younger Dryas (YD), during which the microcharcoal accumulation rates were relatively low.

exposure time) have substantially changed through the sediment core. When the effect of degradation (section 3.3) is minor, the LVG/(LVG + PAHs) ratio represents the relative intensity of past fires recorded in marine sediments: High (low) intensity fires produce high (low) relative abundances of PAHs but low (high) relative abundances of levoglucosan (Wang et al., 2017).

To calculate the LVG/(LVG + PAHs) ratio, the concentration of levoglucosan/PAHs is firstly normalized in the same range of 0 to 1, respectively:

$$Norm_{LVG} = \frac{X}{X_{max} - X_{min}}$$

$$Norm_{PAHs} = \frac{Y}{Y_{max} - Y_{min}}$$

X_{max}/X_{min} represents the maximum/minimum concentration of levoglucosan in the sediment core; Y_{max}/Y_{min} represents the maximum/minimum total concentration sum of PAHs in the sediment core. Then the ratio LVG/(LVG + PAHs) is calculated based on $Norm_{LVG}$ and $Norm_{PAHs}$. A ratio of 0.5 is a boundary: Ratios <0.5 represent a major contribution of PAHs (high intensity fires); ratios >0.5 reflect a major contribution of levoglucosan (low intensity fires).

Microcharcoal particles are produced by both low intensity and high intensity, the accumulation rate of which thus indicates general fire occurrence. Together with the LVG/(LVG + PAHs) ratio, past fire regime in East Java over the past 22,000 years is reconstructed. Proxies for hydroclimate and vegetation from the same sediment core are compared (Ruan et al., 2019). The proxies include the lithogenic particles to $CaCO_3$ ratio and the leaf wax δD (stable hydrogen isotope composition) reflecting riverine runoff and wet season rainfall intensity in East Java, respectively (Mohtadi et al., 2011; Ruan et al., 2019). The leaf wax $\delta^{13}C$ (stable carbon isotope composition) and pollen percentages reflect regional vegetation changes (Ruan et al., 2019). Specifically, $\delta^{13}C_{n\text{-}33}$ (the $\delta^{13}C$ value of leaf wax n-C_{33} alkane) predominantly reflects the contribution of C_3 versus C_4 plant types in East Javanese lowland vegetation; higher values indicate C_4 grass (savannah) expansion at the cost of lowland rainforest (Ruan et al., 2019). The δD value of leaf wax n-C_{33} alkane ($\delta D_{n\text{-}33}$) predominantly reflects wet season rainfall intensity in the East Javanese lowlands (Ruan et al., 2019).

3. Results

3.1. Pyrogenic Source of PAHs

The IP/(IP + BghiP) ratios through the sediment core remain higher than 0.2 (section 2.4; Figure S1), indicating that the PAHs analyzed are mainly pyrogenic. The minor input from petroleum is also supported by the relatively high carbon preference index (CPI) values of the n-alkanes throughout the core (Ruan et al., 2019).

3.2. Accumulation Rate of Microcharcoal, Levoglucosan, and PAHs

In sediment core GeoB10053-7, the highest accumulation rates of microcharcoal particles (Figure 2f) occurred during the LGM. They displayed millennial-scale variations during the deglaciation, with peaks in the Bølling-Allerød (B-A, 14.6–12.9 ka) but low values during the Heinrich Stadial 1 (HS1, 17.5–14.6 ka) and less prominently the Younger Dryas (YD, 12.9–11.6 ka) (ka: thousand years ahead of 1950 AD; chronology based on Svensson et al., 2008, and Cheng et al., 2016). According to the microcharcoal accumulation rates we divide the Holocene into two parts, with low values during the early Holocene (10 to 3 ka) and high values during the late Holocene (3 ka till now).

The peak of levoglucosan in the chromatography of each sediment sample has a distinct peak shape and thus high signal to noise ratio. The detection limit during the analyses was 12.5 pg on column. The lowest measured value among all the samples was 103 pg on column, much higher than the detection limit. The levoglucosan accumulation rates showed a general increase through the sediment core, similar with the trend of sedimentation rates (Figures 2d and 2h). In contrast, there is a clear LGM-Holocene contrast in the accumulation rates of the PAHs, with high fluxes for the LGM part but low fluxes for the early

Holocene part (Figure 2e). Despite the relatively low sedimentation rates during the LGM, the high concentrations of all seven PAHs resulted in high accumulation rates during that period (Figure S1).

3.3. Minor Effect of Degradation on Levoglucosan and LVG/(LVG + PAHs) Ratio

Sedimentation rate potentially impacts the sedimentary levoglucosan concentrations since faster sediment burial leads to shorter oxygen exposure time and better preservation (Hartnett et al., 1998). However, the very weak correlation between levoglucosan concentrations and sedimentation rates from the sediment core ($R = 0.040$, $p = 0.745$) rules out this impact. Levoglucosan may also be prone to post-depositional degradation, although the knowledge of its impact on levoglucosan concentrations over long time scales is limited (Suciu et al., 2019). Levoglucosan is detected in considerable concentrations in sediments dating back to 200 ka (Schreuder et al., 2019), 270 ka (Elias et al., 2001), and 430 ka (Dietze et al., 2020), suggesting its long lifetime in sedimentary environments after deposition, possibly related to the adsorption to biogenic particles proposed by Schreuder et al. (2018). The postdepositional degradation of levoglucosan cannot be completely ruled out but is expected to have minor impact on the downcore variation in our record. Therefore, we infer a minor effect of degradation on levoglucosan concentrations and the ratio of levoglucosan over PAHs in sediment core GeoB10053–7.

The LVG/(LVG + PAHs) ratio was generally lower than 0.5 during the LGM and higher than 0.5 after the LGM (Figure 2g).

4. Discussion

4.1. LGM

High fire occurrence in East Java during the LGM is indicated by high abundances of microcharcoal particles (Figure 2f), with the dominance of high intensity fires as revealed by the low LVG/(LVG + PAHs) values (Figure 2g). Thus, the fire regime during that period was characterized by frequent intense fires.

The vegetation reconstruction from the same sediment core shows that extensive C_4 grasses in East Javanese lowlands were present during the LGM (Ruan et al., 2019; Figure 2a). According to ecosystem-scale burning experiments, the LVG/(LVG + PAHs) values should be higher with grass expansion (Wang et al., 2017). However, low LVG/(LVG + PAHs) values are observed in our record for the LGM, which cannot be explained by the change in vegetation types but supports our interpretation of LVG/(LVG + PAHs) reflecting fire intensity. The frequent and intense fire regime effectively limited tree cover and maintained an open canopy vegetation. As a positive feedback, the presence of a grassy ground layer significantly increases the flammability of the ecosystem; grasses regrow and regain the flammability quickly after burning, allowing frequent and high intensity fires to occur (Bond, 2008; Hoffmann, Geiger, et al., 2012; Stott, 2000).

Proxies from the sediment core indicate that the runoff remained intermediate during the LGM (Figure 2c) while the wet season rainfall was intensified in East Java lowlands (Figure 2b). Consequently, strong rainfall seasonality prevailed during that period, with a long dry season and a short but intense wet season (Ruan et al., 2019). The pronounced rainfall seasonality favored an increase in both fire frequency and intensity. Satellite observations show that more frequent fires occur in years with extended dry seasons, which more efficiently dry out potential fuels and make them prone to ignition (Van der Werf et al., 2008). Fire experiments in savannah ecosystems observe high fire intensity when the fuel moisture content is low (Govender et al., 2006). The short but intense wet season likely facilitated the rapid regrowth of grasses, producing enough potential fuel for frequent fires in the dry season.

4.2. The Deglaciation

A shift in regional fire regime occurred around 18 ka: A substantial decrease in both fire occurrence and fire intensity occurred, reflected by a drop in the accumulation rate of microcharcoal particles and a rise of LVG/(LVG + PAHs) (Figures 2f and 2g). While the fire intensity remained generally low during the deglaciation (Figure 2g), millennial-scale oscillations occurred in fire occurrence: Accumulation rates of microcharcoal, levoglucosan and PAHs were relatively high during the B-A but low during the HS1 and less prominantly, the YD (Figures 2d–2f).

The millennial-scale change in fire occurrence coincided with changes in the lowland vegetation of East Java. The vegetation reconstruction shows two major transitions from savannah toward rainforest in

lowland East Java over the course of the HS1 and the YD, with a reverse trend during the B-A (Ruan et al., 2019). Over the course of the HS1 and the YD, a sharp decrease in both fire occurrence and fire intensity compared to the LGM level likely facilitated the change from grass- to tree-dominated vegetation. With the fire intensity remaining low, an increase in fire occurrence during the B-A likely caused a slight increase in grass cover. Such a pattern can be explained by different growth patterns of grasses versus trees. Unlike fast-growing grasses, tree saplings need a fire-free interval to reach certain sizes to escape flame damage of subsequent fires and continue growing (Bond & Midgley, 2000; Hoffmann, Geiger, et al., 2012). Additionally, trees of certain sizes are more likely to survive low intensity fires than high intensity fires (Hoffmann, Geiger, et al., 2012). Therefore, a combination of both low fire occurrence and low fire intensity during the HS1 and the YD was crucial for increasing the survival chances of trees, which was not the case during the B-A. The low intensity fire regime was still able to ignite grasses during the dry season, which potentially created space for trees. The rising atmospheric CO_2 concentration during the HS1 and the YD potentially also facilitated the vegetation transition by accelerating the growth rates of trees (Bond & Midgley, 2000; Harrison & Sanchez Goñi, 2010).

The riverine runoff from East Java during the deglaciation was at a generally similar level as during the LGM, while the wet season rainfall intensity in the lowlands gradually declined as reflected by the rising $\delta D_{n\text{-}33}$ values (Ruan et al., 2019). Consequently, the lowland dry (fire) season was getting shorter in the course of the deglaciation, which dried out potential fuels less efficiently. On the millennial time scale, there was more runoff during the B-A than during the HS1 and the YD (Figure 2c; Mohtadi et al., 2011). The $\delta D_{n\text{-}33}$ values for the B-A sediments were relatively low (Figure 2b), implying that intense rainfall in the wet season caused the enhanced runoff during that period. The intense wet season likely increased the grass fuel load that were prone to ignite during the dry season.

4.3. Holocene

Fire occurrence was generally low in East Java at the onset of the Holocene before a rise from ~3 ka onward as reflected by microcharcoal accumulation rates (Figure 2f). The fire intensity remained generally constant through the Holocene, since the LVG/(LVG + PAHs) ratios rarely fell below 0.5 (Figure 2g).

During the early Holocene, rainforest continued to replace grass and became widespread both in lowland and montane areas of East Java (Ruan et al., 2019). The rainforest dominated vegetation coincided with rare fires of low intensity. The dense canopy of tropical rainforest suppresses fires by reducing grass fuel loads and maintaining a humid and low-wind microclimate (Hoffmann, Jaconis, et al., 2012). Since ~3 ka, however, C_4 grass expanded at the expense of rainforest in the East Javanese lowlands, while fire occurrence also increased (Figure 2a).

Rainfall intensity of the wet season in East Java through the Holocene was generally low except for a peak at ~2 ka as reflected by the $\delta D_{n\text{-}33}$ values (Figure 2b), while the runoff was intermediate during the early Holocene and increased after ~3 ka (Figure 2c) (Ruan et al., 2019). These proxies indicate a moist early Holocene climate with low rainfall seasonality, making it difficult for fuels to dry sufficiently for ignition.

In assessing the fire history of East Java during the late Holocene, human influences have to be considered. Humans affect fire occurrence in either a positive or a negative way, by increasing ignition or supressing/eliminating fires (Whitlock et al., 2010). Modern humans are believed to have been present in East Java since at least the LGM, based on findings of human skull fragments dated back to 37–29 ka by an archeological study in East Java (Storm et al., 2013). Pottery fragments first appeared around 4.7 ka, and their numbers started to increase around 2.6 ka in a cave in Southeast Java, implying intensified human activity and use of fire (Morwood et al., 2008). The increase in fire occurrence and expansion of lowland C_4 grass since ~3 ka could be related to anthropogenic burning practices, which are generally more frequent than naturally occurring fires (Veenendaal et al., 2018). However, the spatial extent of human impact remains unknown, which makes it difficult to attribute the regional signal recorded in our sediment core to human activity.

4.4. Feedbacks

The results from our study show a strong feedback loop between regional fire regime and mosaic lowland rainforest-savannah vegetation over the past 22,000 years (black loop in Figure 3), while regional rainfall seasonality exerted an impact on both (blue arrows in Figure 3).

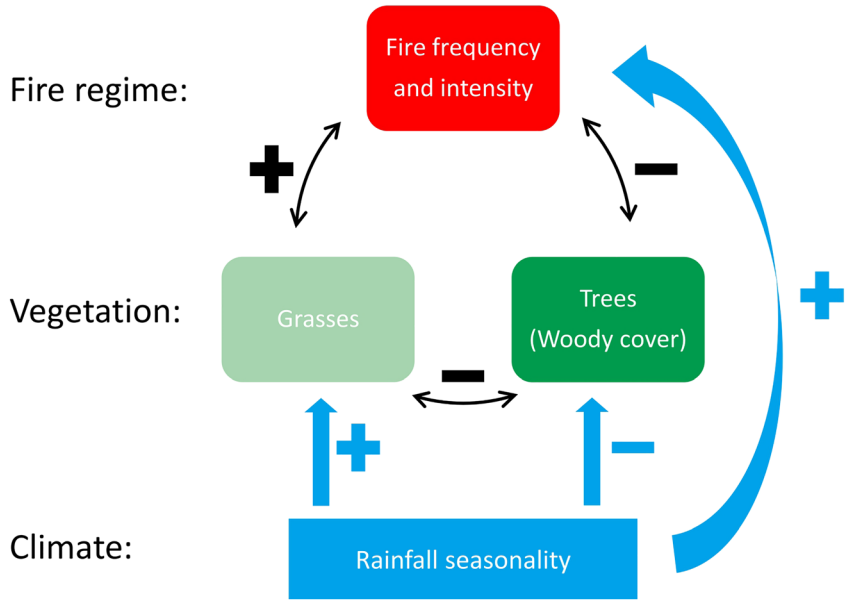

Figure 3. Conceptual diagram illustrating the interaction between fire regime, vegetation, and climate (positive impact: +; negative impact: −). The feedbacks between fire and vegetation, composed of trees and grasses, are shown in the black loop. For example, tree growth is impeded by more frequent and/or intense fires (negative impact); a decrease in woody cover allows an increase in grass cover (negative relation); the flammable grasses lead to an increase in fire frequency and/or intensity (positive impact). Rainfall seasonality serves as a first order control on both fire regime and vegetation (blue arrows). Seasonal drought limits tree growth and canopy closure (negative impact) but efficiently dry out fuels for fires (positive impact); intense wet season facilitate fast growth of grasses (positive impact), providing enough fuels for fires (positive impact).

A series of feedbacks maintained two alternative stable ecosystems in East Java lowlands: savannah-dominated vegetation during the LGM and rainforest-dominated vegetation during the early Holocene. During the LGM, fires of high frequency and intensity impeded the growth of tree saplings and created space for grasses. The highly flammable nature of C_4 grasses further enhanced this fire regime (Bond, 2008; Hoffmann, Geiger, et al., 2012; Stott, 2000). The LGM climate with a drier and longer dry season (Ruan et al., 2019) was a prerequisite for potential fuels to dry out and for frequent fires to occur (Van der Werf et al., 2008). An increase in water stress during the dry season favored expansion of drought tolerant C_4 grasses (Dubois et al., 2014). Meanwhile, the short but intense wet season during the LGM (Ruan et al., 2019) allowed for the quick regrowth of grasses, the retained flammability of which further promotes more fires in the dry season. During the early Holocene, low occurrence of fires with low intensity allowed the growth of trees and the closure of the canopy, limiting the growth of grasses due to low light penetration into the understorey. The climate during the early Holocene was characterized by low rainfall seasonality (Ruan et al., 2019), which favored the tropical rainforest vegetation over savannah (Dubois et al., 2014; Murphy & Bowman, 2012). The relatively evenly distributed rainfall and the rainforest vegetation reduced the amount and the flammability of potential fuels, maintaining a fire regime of low frequency and low intensity (Archibald et al., 2013; Hoffmann, Geiger, et al., 2012). A similar coupling of vegetation changes and fire occurrence is recorded in several tropical lowland sites, that is, a swamp in West Java (Van der Kaars et al., 2001), lakes in Sulawesi (Hamilton et al., 2019), and West Africa (Shanahan et al., 2016), respectively. These records indicate that high representation of grass corresponded with high fire occurrence, although fire intensity was not resolved in those studies.

During the deglaciation and the late Holocene, the above feedbacks were disturbed. Under changing rainfall seasonality, fires played an important role in changing vegetation between the two stable states earlier described. Different combinations of frequency and intensity of fires determined whether trees could escape the "fire trap" and compete with grasses, which led to a shift in regional vegetation cover. A fire regime of low intensity but high frequency during the B-A and the late Holocene was concurrent with C_4 grass expansion, implying that such a fire regime was still strong enough to ignite both trees and grasses. In contrast, a

fire regime of low frequency and low intensity during the HS1 (and less prominantly, the YD) potentially facilitated the change from savannah-dominated vegetation to rainforest-dominated vegetation by selectively clearing grasses and creating space for trees. As a feedback, the gradual increase in tree cover at the expense of lowland C_4 grasses reduced the availability of a flammable grass layer for fires to spread, which further decreased regional fire occurrence. Such a fire regime is an analogue for that in West Africa during the early Holocene (Dupont & Schefuß, 2018) and that in Southwest Africa during the late Miocene (Hoetzel et al., 2013). Fire disturbance during the African Humid Period likely created a mosaic vegetation structure and facilitated high density of woody species (Dupont & Schefuß, 2018).

Our results indicate that rainfall seasonality has been a first order control on fire regime and vegetation changes in East Java since the LGM. They are consistent with findings from other studies that enhanced rainfall seasonality has a two-fold effect of maintaining savannah by reducing tree growth and canopy closure while increasing the probability of fire occurrence (Lehmann et al., 2011). High rainfall seasonality significantly increases the fire frequency in regions experiencing high annual rainfall by drying out large quantities of fuels and limiting tree cover (Staal et al., 2018). Our multiproxy study indicates the importance of rainfall seasonality in modifying fire regime and vegetation types over a broad region and on long periods. An amplified rainfall seasonality was present in the southern part of the Maritime Continent (from southern Indonesia to northern Australia) during the LGM, as shown by a multimodel numerical simulation of the Australian-Indonesian monsoon system (Yan et al., 2018). The exposure of the Sunda and Sahul Shelves during the LGM played an important role by changing regional atmospheric circulation (DiNezio et al., 2016): Weakened upward air mass motion in austral winter decreased dry season rainfall, while enhanced moisture convergence in austral summer increased wet season rainfall intensity (Yan et al., 2018). Apart from East Java, the expansion of C_4 grass vegetation during the LGM was evident in Sulawesi (Russell et al., 2014; Wicaksono et al., 2015, 2017), southern Borneo (Wurster et al., 2019), and Sumba (Dubois et al., 2014). Fires thus likely also played a significant role in maintaining savannah ecosystems there.

Our results provide a long-term context to assess potential changes in fire regime and tropical ecosystems in the future, a time when human activities are the most extensive and intensive over the past 22,000 years. Under a scenario of continuing anthropogenic greenhouse gas emission, global climate models predict a trend of increasing rainfall seasonality and a more prolonged dry season over most of the tropical regions by the end of the century (Pascale et al., 2016). Such a change would favor higher fire frequency and intensity while threatening tropical forests as shown in the results during the LGM. Moreover, the forest loss in the tropics is increasing by 2,101 square kilometers per year over the 21st Century (Hansen et al., 2013). The increased flammability of the tropical ecosystems due to lower tree covers would make fires more prone to evade control, especially during the dry season. However, this trend could also be slowed by actively reducing fire frequency and intensity via changing burning practices and patterns, since fire exclusion experiments provide evidence of forest encroachment into savannah (Veenendaal et al., 2018).

5. Conclusions

In this study, we present accumulation rates of microcharcoal and two molecular burning markers (levoglucosan and PAHs) from a sediment core covering the past 22,000 years. While the microcharcoal accumulation rate reflects general fire occurrence in East Java, the ratio of levoglucosan versus PAHs indicates relative fire intensity. The regional fire occurrence was highest during the LGM and showed two additional maxima during the Bølling-Allerød and the late Holocene, while the fire level was low during the Heinrich Stadial 1, the Younger Dryas, and the early Holocene. Fire intensity was high during the LGM but remained low since 18 ka. The combination of charcoal and molecular markers shows great potential for detailed paleo-fire regime reconstruction.

A series of feedbacks of fire with hydroclimate and vegetation stablized two alternative stable ecosystems in East Javanese lowlands during the LGM and during the early Holocene, respectively. The LGM was characterized by high rainfall seasonality, high occurrence of intense fires, and savannah-dominated vegetation, while the early Holocene was characterized by low rainfall seasonality, low occurrence of fires of low intensity, and rainforest-dominated vegetation. The deglaciation and the late Holocene were transition periods between the two stable states. A fire regime of low frequency and low intensity during the Heinrich Stadial 1 and the Younger Dryas coincided with major transitions from savannah toward rainforest, while

a reverse change in vegetation during the Bølling-Allerød was concurrent with a fire regime of low intensity but high frequency. Hydroclimatic changes in rainfall seasonality thus have the potential to facilitate large-scale vegetation changes mediated by changes in fire regime. Our results implicate more frequent and intense fires in the future in light of the projected increase in the seasonality of the tropical climate.

Data Availability Statement

Data sets related to this study can be found at PANGAEA repository (https://doi.org/10.1594/PANGAEA.915962).

Acknowledgments

This work was funded through the German Ministry of Education and Research (BMBF) grants 03G0184A (PABESIA) and 03G0864F (CAHOL). Support was provided through the Cluster of Excellence "The Ocean Floor—Earth's Uncharted Interface" in Bremen. Y. R. is funded by CSC—the China Scholarship Council and supported by GLOMAR—Bremen International Graduate School for Marine Sciences. S. vdK. was funded by the Deutsche Forschungsgemeinschaft (DFG) grant BE2116/10-1. S. S. and E. C. H. are supported by the Netherlands Earth System Science Center (NESSC) funded by the Dutch Ministry for Education and Science. E. J. H. acknowledges the support of the NASA FIREX-AQ program, grant NNH17ZDA001N. We thank Ralph Kreutz (MARUM), Denise Dorhout (NIOZ), and Monique Verweij (NIOZ) for laboratory support. Lydia Gerullis is acknowledged for data set preparation. Open access funding enabled and organized by Projekt DEAL.

References

Archibald, S., Lehmann, C., Belcher, C., Bond, W., Bradstock, R., Daniau, A.-L., et al. (2018). Biological and geophysical feedbacks with fire in the Earth system. *Environmental Research Letters*, *13*(3), 033003. https://doi.org/10.1088/1748-9326/aa9ead

Archibald, S., Lehmann, C., Gomez-Dans, J., & Bradstock, R. (2013). Defining pyromes and global syndromes of fire regimes. *Proceedings of the National Academy of Sciences*, *110*(16), 6442–6447. https://doi.org/10.1073/pnas.1211466110

Argiriadis, E., Battistel, D., McWethy, D., Vecchiato, M., Kirchgeorg, T., Kehrwald, N., et al. (2018). Lake sediment fecal and biomass burning biomarkers provide direct evidence for prehistoric human-lit fires in New Zealand. *Scientific Reports*, *8*(1), 1–9. https://doi.org/10.1038/s41598-018-30606-3

Battistel, D., Argiriadis, E., Kehrwald, N., Spigariol, M., Russell, J., & Barbante, C. (2017). Fire and human record at Lake Victoria, East Africa, during the early iron age: Did humans or climate cause massive ecosystem changes? *The Holocene*, *27*(7), 997–1007. https://doi.org/10.1177/0959683616678466

Beaufort, L., de Garidel-Thoron, T., Linsley, B., Oppo, D., & Buchet, N. (2003). Biomass burning and oceanic primary production estimates in the Sulu Sea area over the last 380 kyr and the east Asian monsoon dynamics. *Marine Geology*, *201*(1–3), 53–65. https://doi.org/10.1016/S0025-3227(03)00208-1

Bhattarai, H., Saikawa, E., Wan, X., Zhu, H., Ram, K., Gao, S., et al. (2019). Levoglucosan as a tracer of biomass burning: Recent progress and perspectives. *Atmospheric Research*, *220*, 20–33. https://doi.org/10.1016/j.atmosres.2019.01.004

Bond, W. (2008). What limits trees in C4 grasslands and savannas? *Annual Review of Ecology, Evolution, and Systematics*, *39*(1), 641–659. https://doi.org/10.1146/annurev.ecolsys.39.110707.173411

Bond, W., & Keeley, J. (2005). Fire as a global 'herbivore': The ecology and evolution of flammable ecosystems. *Trends in Ecology & Evolution*, *20*(7), 387–394. https://doi.org/10.1016/j.tree.2005.04.025

Bond, W., & Midgley, G. (2000). A proposed CO_2-controlled mechanism of woody plant invasion in grasslands and savannas. *Global Change Biology*, *6*(8), 865–869. https://doi.org/10.1046/j.1365-2486.2000.00365.x

Bowman, D., Balch, J., Artaxo, P., Bond, W., Carlson, J., Cochrane, M., et al. (2009). Fire in the Earth system. *Science*, *324*(5926), 481–484. https://doi.org/10.1126/science.1163886

Cheng, H., Edwards, R. L., Sinha, A., Spötl, C., Yi, L., Chen, S., et al. (2016). The Asian monsoon over the past 640,000 years and ice age terminations. *Nature*, *534*(7609), 640–646. https://doi.org/10.1038/nature18591

Daniau, A., Harrison, S., & Bartlein, P. (2010). Fire regimes during the Last Slacial. *Quaternary Science Reviews*, *29*(21–22), 2918–2930. https://doi.org/10.1016/j.quascirev.2009.11.008

Daniau, A.-L., Desprat, S., Aleman, J. C., Bremond, L., Davis, B., Fletcher, W., et al. (2019). Terrestrial plant microfossils in palaeoenvironmental studies, pollen, microcharcoal and phytolith. Towards a comprehensive understanding of vegetation, fire and climate changes over the past one million years. *Revue de Micropaleontologie*, *63*, 1–35. https://doi.org/10.1016/j.revmic.2019.02.001

Dietze, E., Brykała, D., Schreuder, L., Jażdżewski, K., Blarquez, O., Brauer, A., et al. (2019). Human-induced fire regime shifts during 19th century industrialization: A robust fire regime reconstruction using northern polish lake sediments. (W. Finsinger, Ed.). *PLoS ONE*, *14*(9), e0222011. https://doi.org/10.1371/journal.pone.0222011

Dietze, E., Mangelsdorf, K., Andreev, A., Karger, C., Schreuder, L. T., Hopmans, E. C., et al. (2020). Relationships between low-temperature fires, climate and vegetation during three late glacials and interglacials of the last 430 kyr in northeastern Siberia reconstructed from monosaccharide anhydrides in Lake El'gygytgyn sediments. *Climate of the Past*, *16*(2), 799–818. https://doi.org/10.5194/cp-16-799-2020

DiNezio, P., Timmermann, A., Tierney, J., Jin, F., Otto-Bliesner, B., Rosenbloom, N., et al. (2016). The climate response of the Indo-Pacific warm pool to glacial sea level. *Paleoceanography*, *31*, 866–894. https://doi.org/10.1002/2015PA002890

Dubois, N., Oppo, D., Galy, V., Mohtadi, M., van Der Kaars, S., Tierney, J., et al. (2014). Indonesian vegetation response to changes in rainfall seasonality over the past 25,000 years. *Nature Geoscience*, *7*(7), 513–517. https://doi.org/10.1038/ngeo2182

Dupont, L., & Schefuß, E. (2018). The roles of fire in Holocene ecosystem changes of West Africa. *Earth and Planetary Science Letters*, *481*, 255–263. https://doi.org/10.1016/j.epsl.2017.10.049

Elias, V. O., Simoneit, B. R. T., Cordeiro, R. C., & Turcq, B. (2001). Evaluating levoglucosan as an indicator of biomass burning in Carajás, Amazônia: A comparison to the charcoal record. *Geochimica et Cosmochimica Acta*, *65*(2), 267–272. https://doi.org/10.1016/s0016-7037(00)00522-6

Giglio, L., Schroeder, W., & Justice, C. (2016). The collection 6 MODIS active fire detection algorithm and fire products. *Remote Sensing of Environment*, *178*, 31–41. https://doi.org/10.1016/j.rse.2016.02.054

Gill, A. (1975). Fire and the Australian flora: A review. *Australian Forestry*, *38*(1), 4–25.

Govender, N., Trollope, W., & van Wilgen, B. (2006). The effect of fire season, fire frequency, rainfall and management on fire intensity in savanna vegetation in South Africa. *Journal of Applied Ecology*, *43*(4), 748–758. https://doi.org/10.1111/j.1365-2664.2006.01184.x

Hamilton, R., Stevenson, J., Li, B., & Bijaksana, S. (2019). A 16,000-year record of climate, vegetation and fire from Wallacean lowland tropical forests. *Quaternary Science Reviews*, *224*, 105929. https://doi.org/10.1016/j.quascirev.2019.105929

Han, Y., Peteet, D., Arimoto, R., Cao, J., An, Z., Sritrairat, S., & Yan, B. (2016). Climate and fuel controls on North American Paleofires: Smoldering to flaming in the Late-Glacial-Holocene transition. *Scientific Reports*, *6*(1), 1–8. https://doi.org/10.1038/srep20719

Hansen, M., Potapov, P., Moore, R., Hancher, M., Turubanova, S., Tyukavina, A., et al. (2013). High-resolution global maps of 21st-century forest cover change. *Science*, *342*(6160), 850–853. https://doi.org/10.1126/science.1244693

Harrison, S. P., & Sanchez Goñi, M. F. (2010). Global patterns of vegetation response to millennial-scale variability and rapid climate change during the last glacial period. *Quaternary Science Reviews*, *29*(21–22), 2957–2980. https://doi.org/10.1016/j.quascirev.2010.07.016

Hartnett, H., Keil, R., Hedges, J., & Devol, A. (1998). Influence of oxygen exposure time on organic carbon preservation in continental margin sediments. *Nature*, *391*(6667), 572–574. https://doi.org/10.1038/35351

Hebbeln, D., & cruise participants (2006). Documentation of sediment core GeoB10053-7. PANGAEA. https://doi.org/10.1594/PANGAEA.394421

Hirota, M., Holmgren, M., van Nes, E., & Scheffer, M. (2011). Global resilience of tropical forest and savanna to critical transitions. *Science (New York, N.Y.)*, *334*(6053), 232–235. https://doi.org/10.1126/science.1210657

Hoetzel, S., Dupont, L., Schefuß, E., Rommerskirchen, F., & Wefer, G. (2013). The role of fire in Miocene to Pliocene C4 grassland and ecosystem evolution. *Nature Geoscience*. https://doi.org/10.1038/NGEO1984

Hoffmann, W., Geiger, E., Gotsch, S., Rossatto, D., Silva, L., Lau, O., et al. (2012). Ecological thresholds at the savanna-forest boundary: How plant traits, resources and fire govern the distribution of tropical biomes. *Ecology Letters*, *15*(7), 759–768. https://doi.org/10.1111/j.1461-0248.2012.01789.x

Hoffmann, W., Jaconis, S., Mckinley, K., Geiger, E., Gotsch, S., & Franco, A. (2012). Fuels or microclimate? Understanding the drivers of fire feedbacks at savanna-forest boundaries. *Austral Ecology*, *37*(6), 634–643. https://doi.org/10.1111/j.1442-9993.2011.02324.x

Hunsinger, G., Mitra, S., Warrick, J., & Alexander, C. (2008). Oceanic loading of wildfire-derived organic compounds from a small mountainous river. *Journal of Geophysical Research*, *113*, G02007. https://doi.org/10.1029/2007JG000476

Kalnay, E., Kanamitsu, M., Kistler, R., Collins, W., Deaven, D., Gandin, L., et al. (1996). The NCEP/NCAR 40-year reanalysis project. *Bulletin of the American Meteorological Society*, *77*(3), 437–471. https://doi.org/10.1175/1520-0477(1996)077<0437:TNYRP>2.0.CO;2

Keiluweit, M., Kleber, M., Sparrow, M., Simoneit, B., & Prahl, F. (2012). Solvent-extractable polycyclic aromatic hydrocarbons in biochar: In fl uence of pyrolysis temperature and feedstock. *Environmental Science & Technology*, *46*(17), 9333–9341. https://doi.org/10.1021/es302125k

Kuo, L.-J., Herbert, B., & Louchouarn, P. (2008). Can levoglucosan be used to characterize and quantify char/charcoal black carbon in environmental media? *Organic Geochemistry*, *39*(10), 1466–1478. https://doi.org/10.1016/J.ORGGEOCHEM.2008.04.026

Lehmann, C., Archibald, S., Hoffmann, W., & Bond, W. (2011). Deciphering the distribution of the savanna biome. *New Phytologist*, *191*(1), 197–209. https://doi.org/10.1111/j.1469-8137.2011.03689.x

Lima, A., Farrington, J., & Reddy, C. (2005). Combustion-derived polycyclic aromatic hydrocarbons in the environment—A review. *Environmental Forensics*, *6*(2), 109–131. https://doi.org/10.1080/15275920590952739

Lu, H., Zhu, L., & Zhu, N. (2009). Polycyclic aromatic hydrocarbon emission from straw burning and the influence of combustion parameters. *Atmospheric Environment*, *43*(4), 978–983. https://doi.org/10.1016/j.atmosenv.2008.10.022

Miller, D., Castañeda, I., Bradley, R., & MacDonald, D. (2017). Local and regional wildfire activity in central Maine (USA) during the past 900 years. *Journal of Paleolimnology*, *58*(4), 455–466. https://doi.org/10.1007/s10933-017-0002-z

Mohtadi, M., Oppo, D., Steinke, S., Stuut, J., De Pol-Holz, R., Hebbeln, D., & Lückge, A. (2011). Glacial to Holocene swings of the Australian-Indonesian monsoon. *Nature Geoscience*, *4*(8), 540–544. https://doi.org/10.1038/ngeo1209

Morwood, M., Sutikna, T., Saptomo, E., Westaway, K., Jatmiko, Due, R. A., et al. (2008). Climate, people and faunal succession on Java, Indonesia: Evidence from Song Gupuh. *Journal of Archaeological Science*, *35*(7), 1776–1789. https://doi.org/10.1016/j.jas.2007.11.025

Murphy, B., & Bowman, D. (2012). What controls the distribution of tropical forest and savanna? *Ecology Letters*, *15*(7), 748–758. https://doi.org/10.1111/j.1461-0248.2012.01771.x

Myers-Pigg, A., Louchouarn, P., & Teisserenc, R. (2017). Flux of dissolved and particulate low-temperature pyrogenic carbon from two high-latitude rivers across the spring freshet hydrograph. *Frontiers in Marine Science*, *4*. https://doi.org/10.3389/fmars.2017.00038

Ondei, S., Prior, L., Williamson, G., Vigilante, T., & Bowman, D. (2017). Water, land, fire, and forest: Multi-scale determinants of rainforests in the Australian monsoon tropics. *Ecology and Evolution*, *7*(5), 1592–1604. https://doi.org/10.1002/ece3.2734

Pascale, S., Lucarini, V., Feng, X., Porporato, A., & ul Hasson, S. (2016). Projected changes of rainfall seasonality and dry spells in a high greenhouse gas emissions scenario. *Climate Dynamics*, *46*(3–4), 1331–1350. https://doi.org/10.1007/s00382-015-2648-4

Ramanathan, V., Crutzen, P., Kiehl, J., & Rosenfeld, D. (2001). Atmosphere: Aerosols, climate, and the hydrological cycle. *Science*, *294*(5549), 2119–2124. https://doi.org/10.1126/science.1064034

Reid, J., Xian, P., Hyer, E., Flatau, M., Ramirez, E., Turk, F., et al. (2012). Multi-scale meteorological conceptual analysis of observed active fire hotspot activity and smoke optical depth in the Maritime Continent. *Atmospheric Chemistry and Physics*, *12*(4), 2117–2147. https://doi.org/10.5194/acp-12-2117-2012

Ruan, Y., Mohtadi, M., van der Kaars, S., Dupont, L., Hebbeln, D., & Schefuß, E. (2019). Differential hydro-climatic evolution of east Javanese ecosystems over the past 22,000 years. *Quaternary Science Reviews*, *218*, 49–60. https://doi.org/10.1016/j.quascirev.2019.06.015

Russell, J., Vogel, H., Konecky, B., Bijaksana, S., Huang, Y., Melles, M., et al. (2014). Glacial forcing of central Indonesian hydroclimate since 60,000 y B.P. *Proceedings of the National Academy of Sciences*, *111*(14), 5100–5105. https://doi.org/10.1073/pnas.1402373111

Santín, C., Doerr, S., Kane, E., Masiello, C., Ohlson, M., de la Rosa, J., et al. (2016). Towards a global assessment of pyrogenic carbon from vegetation fires. *Global Change Biology*, *22*(1), 76–91. https://doi.org/10.1111/gcb.12985

Schkolnik, G., & Rudich, Y. (2006). Detection and quantification of levoglucosan in atmospheric aerosols: A review. *Analytical and Bioanalytical Chemistry*, *385*(1), 26–33. https://doi.org/10.1007/s00216-005-0168-5

Schreuder, L., Donders, T., Mets, A., Hopmans, E., Sinninghe Damsté, J., & Schouten, S. (2019). Comparison of organic and palynological proxies for biomass burning and vegetation in a lacustrine sediment record (Lake Allom, Fraser Island, Australia). *Organic Geochemistry*, *133*. https://doi.org/10.1016/j.orggeochem.2019.03.002

Schreuder, L., Hopmans, E., Stuut, J., Sinninghe Damsté, J., & Schouten, S. (2018). Transport and deposition of the fire biomarker levoglucosan across the tropical North Atlantic Ocean. *Geochimica et Cosmochimica Acta*, *227*, 171–185. https://doi.org/10.1016/j.gca.2018.02.020

Schüpbach, S., Kirchgeorg, T., Colombaroli, D., Beffa, G., Radaelli, M., Kehrwald, N., & Barbante, C. (2015). Combining charcoal sediment and molecular markers to infer a Holocene fire history in the Maya Lowlands of Petén, Guatemala. *Quaternary Science Reviews*, *115*, 123–131. https://doi.org/10.1016/j.quascirev.2015.03.004

Shanahan, T., Hughen, K., McKay, N., Overpeck, J., Scholz, C., Gosling, W., et al. (2016). CO_2 and fire influence tropical ecosystem stability in response to climate change. *Scientific Reports*, *6*(1), 29587. https://doi.org/10.1038/srep29587

Sikes, E., Medeiros, P., Augustinus, P., Wilmshurst, J., & Freeman, K. (2013). Seasonal variations in aridity and temperature characterize changing climate during the last deglaciation in New Zealand. *Quaternary Science Reviews*, *74*, 245–256. https://doi.org/10.1016/j.quascirev.2013.01.031

Simoneit, B., Schauer, J., Nolte, C., Oros, D., Elias, V., Fraser, M., et al. (1999). Levoglucosan, a tracer for cellulose in biomass burning and atmospheric particles. *Atmospheric Environment*, *33*(2), 173–182. https://doi.org/10.1016/S1352-2310(98)00145-9

Staal, A., van Nes, E., Hantson, S., Holmgren, M., Dekker, S., Pueyo, S., et al. (2018). Resilience of tropical tree cover: The roles of climate, fire, and herbivory. *Global Change Biology*, *24*(11), 5096–5109. https://doi.org/10.1111/gcb.14408

Staver, A., Archibald, S., & Levin, S. (2011). The global extent and determinants of savanna and forest as alternative biome states. *Science*, *334*(6053), 230–232. https://doi.org/10.1126/science.1210465

Storm, P., Wood, R., Stringer, C., Bartsiokas, A., de Vos, J., Aubert, M., et al. (2013). U-series and radiocarbon analyses of human and faunal remains from Wajak, Indonesia. *Journal of Human Evolution*, *64*(5), 356–365. https://doi.org/10.1016/j.jhevol.2012.11.002

Stott, P. (2000). Progress in physical geography combustion in tropical biomass fires: A critical review. *Progress in Physical Geography*. https://doi.org/10.1177/030913330002400303

Suciu, L., Masiello, C., & Griffin, R. (2019). Anhydrosugars as tracers in the Earth system. *Biogeochemistry*, *146*(3), 209–256. https://doi.org/10.1007/s10533-019-00622-0

Svensson, A., Andersen, K. K., Bigler, M., Clausen, H. B., Dahl-Jensen, D., Davies, S. M., et al. (2008). A 60 000 year Greenland stratigraphic ice core chronology. *Climate of the Past*, *4*(1), 47–57. https://doi.org/10.5194/cp-4-47-2008

Tobiszewski, M., & Namieśnik, J. (2012). PAH diagnostic ratios for the identification of pollution emission sources. *Environmental Pollution*, *162*, 110–119. https://doi.org/10.1016/j.envpol.2011.10.025

van der Kaars, S., Miller, G. H., Turney, C. S. M., Cook, E. J., Nürnberg, D., Schönfeld, J., et al. (2017). Humans rather than climate the primary cause of Pleistocene megafaunal extinction in Australia. *Nature Communications*, *8*(1), 14142. https://doi.org/10.1038/ncomms14142

van der Kaars, S., Penny, D., Tibby, J., Fluin, J., Dam, R., & Suparan, P. (2001). Late quaternary palaeoecology, palynology and palaeolimnology of a tropical lowland swamp: Rawa Danau, West-Java, Indonesia. *Palaeogeography, Palaeoclimatology, Palaeoecology*, *171*(3–4), 185–212. https://doi.org/10.1016/S0031-0182(01)00245-0

van der Kaars, S., Wang, X., Kershaw, P., Guichard, F., & Setiabudi, D. A. (2000). A Late Quaternary palaeoecological record from the Banda Sea, Indonesia: Patterns of vegetation, climate and biomass burning in Indonesia and northern Australia. *Palaeogeography, Palaeoclimatology, Palaeoecology*, *155*(1–2), 135–153. https://doi.org/10.1016/S0031-0182(99)00098-X

van der Werf, G., Dempewolf, J., Trigg, S., Randerson, J., Kasibhatla, P., Giglio, L., et al. (2008). Climate regulation of fire emissions and deforestation in equatorial Asia. *Proceedings of the National Academy of Sciences*, *105*(51), 20,350–20,355. https://doi.org/10.1073/pnas.0803375105

Veenendaal, E., Torello-Raventos, M., Miranda, H., Sato, N., Oliveras, I., van Langevelde, F., et al. (2018). On the relationship between fire regime and vegetation structure in the tropics. *New Phytologist*, *218*(1), 153–166. https://doi.org/10.1111/nph.14940

Wakeham, S., Schaffner, C., & Giger, W. (1980). Poly cyclic aromatic hydrocarbons in recent lake sediments—II. Compounds derived from biogenic precursors during early diagenesis. *Geochimica et Cosmochimica Acta*, *44*(3), 415–429. https://doi.org/10.1016/0016-7037(80)90041-1

Wang, X., Thai, P., Mallet, M., Desservettaz, M., Hawker, D., Keywood, M., et al. (2017). Emissions of selected semivolatile organic chemicals from forest and savannah fires. *Environmental Science & Technology*, *51*(3), 1293–1302. https://doi.org/10.1021/acs.est.6b03503

Whitlock, C., Higuera, P., Mcwethy, D., & Briles, C. (2010). Paleoecological perspectives on fire ecology: Revisiting the fire-regime concept. *The Open Ecology Journal*, *3*, 6–23. https://doi.org/10.2174/1874213001003020006

Whitlock, C., & Larsen, C. (2002). In C. Whitlock & C. Larsen. *Charcoal as a fire proxy*. Dordrecht: Springer. https://doi.org/10.1007/0-306-47668-1_5

Wicaksono, S., Russell, J., & Bijaksana, S. (2015). Compound-specific carbon isotope records of vegetation and hydrologic change in central Sulawesi, Indonesia, since 53,000 yr BP. *Palaeogeography, Palaeoclimatology, Palaeoecology*, *430*, 47–56. https://doi.org/10.1016/j.palaeo.2015.04.016

Wicaksono, S., Russell, J., Holbourn, A., & Kuhnt, W. (2017). Hydrological and vegetation shifts in the Wallacean region of central Indonesia since the last glacial maximum. *Quaternary Science Reviews*, *157*, 152–163. https://doi.org/10.1016/j.quascirev.2016.12.006

Wurster, C., Rifai, H., Zhou, B., Haig, J., & Bird, M. (2019). Savanna in equatorial Borneo during the late Pleistocene. *Scientific Reports*, *9*(1), 1–7. https://doi.org/10.1038/s41598-019-42670-4

Yan, M., Wang, B., Liu, J., Zhu, A., Ning, L., & Cao, J. (2018). Understanding the Australian monsoon change during the Last Glacial Maximum with a multi-model ensemble. *Climate of the Past*, *14*(12), 2037–2052. https://doi.org/10.5194/cp-14-2037-2018

Yunker, M., Macdonald, R., Vingarzan, R., Mitchell, R., Goyette, D., & Sylvestre, S. (2002). PAHs in the Fraser River basin: A critical appraisal of PAH ratios as indicators of PAH source and composition. *Organic Geochemistry*, *33*(4), 489–515. https://doi.org/10.1016/S0146-6380(02)00002-5